Geochemical Perspectives Letters

Oxidation of green rust by anoxygenic phototrophic Fe(II)-oxidising bacteria

X. Han[1,2,3,4,5], E.J. Tomaszewski[2], J. Sorwat[2], Y. Pan[1,3,4,5], A. Kappler[2*], J.M. Byrne[2]

doi: 10.7185/geochemlet.2004

Abstract

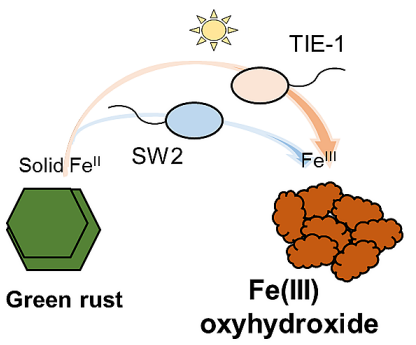

Green rust (GR) may have been a primary mineral phase during the deposition of Fe(III) (oxyhydr)oxides in Precambrian iron formations (IFs). However, the transformation pathways of GR into secondary mineral phases in IFs remain unclear. One potentially relevant mechanism on early Earth is anoxygenic phototrophic microbial oxidation of either dissolved Fe(II) or Fe(II)-bearing minerals that leads to the formation of Fe(III) (oxyhydr)oxides. It is currently unknown whether phototrophic Fe(II)-oxidisers can access lattice Fe(II) in GR. Here, we studied microbial Fe(II) oxidation of carbonate green rust by two anoxygenic phototrophic Fe(II)-oxidising bacteria, *Rhodobacter ferrooxidans* SW2 and *Rhodopseudomonas palustris* TIE-1. We found that these two species could oxidise GR to a short range ordered Fe(III) oxyhydroxide, likely ferrihydrite, with faster GR oxidation rates by SW2 than by TIE-1. These results suggest that anoxygenic phototropic Fe(II) oxidation of GR can contribute to the formation of Fe(III) (oxyhydr)oxides and thus, this process could have been an important mechanism for Precambrian IFs deposition in ancient oceans.

Received 29 May 2019 | Accepted 13 December 2019 | Published 31 January 2020

Introduction

Green rust (GR) is a mixed-valent Fe(II)/Fe(III) mineral, generally described by the formula $[Fe(II)_{1-x}Fe(III)_x(OH)_2]^{x+}[(x/n)A^{n-}, mH_2O]^{x-}$, with A^{n-} denoting intercalated anions and x representing the molar fraction of trivalent cations. It is a product of steel corrosion in O_2-poor environments and is present in Fe-rich sediments (Trolard *et al.*, 1997; Refait *et al.*, 2003; Zegeye *et al.*, 2012). Several studies have suggested GR may have been a potential precursor mineral during the precipitation of Fe(III) (oxyhydr)oxides and even magnetite (Fe_3O_4) in iron formation (IF) deposition (Halevy *et al.*, 2017; Li *et al.*, 2017; Koeksoy *et al.*, 2019). The majority of these Fe-rich rock formations were deposited between 2.80-1.85 Ga in the Neoarchean and Palaeoproterozoic (Klein, 2005) and typically contain iron-bearing minerals such as magnetite and hematite (Konhauser *et al.*, 2017). However, the transformation pathways of GR into secondary mineral phases in IFs remain unclear.

Abiotic O_2-driven Fe(II) oxidation and biotic anoxygenic Fe(II) photosynthesis result in Fe(III) mineral formation in Archean ocean analogues (Wu *et al.*, 2014; Field *et al.*, 2016). These same mechanisms could also contribute to the transformation of GR into the final mineral assemblage in IFs. Microbial transformation of GR by dissolved oxygen and/or nitrate reducing bacteria can lead to the formation of a variety of Fe minerals such as magnetite, ferrihydrite ($Fe_{10}O_{14}(OH)_2$), lepidocrocite (γ-FeOOH) and goethite (α-FeOOH). All of these phases are either found in IFs, or are thought to have been precursor minerals that underwent secondary transformation to the mineral phases observed today (Legrand *et al.*, 2004; Pantke *et al.*, 2012; Miot *et al.*, 2014). Yet, the most likely explanation for IF deposition in a stratified ancient ocean and the absence of Fe in Precambrian surface waters is anoxygenic Fe(II) photosynthesis, based on molecular phylogenetic evidence, Fe(II) oxidation rates by anoxygenic photosynthetic bacteria, and geochemical analyses from IFs (Konhauser *et al.*, 2002; Kappler *et al.*, 2005; Xiong, 2007). What remains unclear, is if phototrophic Fe(II) oxidisers can oxidise GR.

Here, we studied the microbial Fe(II) oxidation of carbonate GR (CO_3^{2-}) by two anoxygenic phototrophic Fe(II)-oxidising bacteria: *Rhodobacter ferrooxidans* SW2 and *Rhodopseudomonas palustris* TIE-1. We investigated the ability of these two species to oxidise Fe(II) in GR by quantifying

1. Biogeomagnetism Group, Key Laboratory of Earth and Planetary Physics, Institute of Geology and Geophysics, Chinese Academy of Sciences, Beijing 100029, China
2. Geomicrobiology, Center for Applied Geosciences, University of Tuebingen, 72074 Tuebingen, Germany
3. France-China International Laboratory of Evolution and Development of Magnetotactic Multicellular Organisms, Chinese Academy of Sciences, Beijing 100029, China
4. Institutions of Earth Science, Chinese Academy of Sciences, China
5. University of Chinese Academy of Sciences, Beijing 100049, China
* Corresponding author (email: andreas.kappler@uni-tuebingen.de)

Fe(II) and total Fe in both aqueous and solid phases spectrophotometrically, and by Mössbauer spectroscopy. We also observed the cell mineral associations using SEM. Based on our results, we hypothesise that anoxygenic phototropic Fe(II) oxidation of GR could have contributed to the formation of Fe(III) (oxyhydr)oxides during Precambrian IFs deposition.

Materials and Methods

GR (CO_3^{2-}) synthesis. GR (CO_3^{2-}) was synthesised following the modified protocol of Bocher *et al.* (2004), (further details in SI). After synthesis, the initial GR was divided into separate bottles, which were washed with anoxic ultrapure H_2O water (GR_water), SW2 medium (GR_SW2) and TIE-1 medium (GR_TIE-1), respectively, in a glovebox to remove dissolved Fe(II).

Culturing medium and experimental setup. Detailed information on cultivation of SW2 and TIE-1 is provided in the SI. Before inoculation, GR_SW2, and GR_TIE-1 stock solution (~6 mM solid Fe(II)) were injected into the 25 ml anoxic and sterile medium. From the stock culture, 10 % (2.5 ml) and 20 % (5 ml) inoculum were added to respective microcosms and incubated for 19 days at 20 °C and 12 µmol quanta $m^{-2}s^{-1}$ (600 lux) with a 40 W tungsten incandescent light bulb. Triplicates were prepared for both SW2 and TIE-1, with an additional sterile setup containing no inoculum to confirm the absence of chemical oxidation of Fe(II).

Fe speciation analysis. For Fe(II) and total Fe (Fe(II) and Fe(III)) analyses in both aqueous and solid phases, 1 ml of culture slurry was centrifuged at 13400 rpm for 10 min. The supernatant was mixed with 1 M HCl to prevent further oxidation. The residual precipitate was dissolved in 6 M HCl within 24 hours, and further diluted with 1 M HCl to prevent Fe(II) oxidation (Porsch and Kappler, 2011). All sampling, centrifugation and dissolution steps were conducted in an anoxic glovebox (100 % N_2). Both Fe(II) and total Fe concentrations were quantified by the ferrozine assay (Stookey, 1970) with Fe(III) calculated as the difference between Fe(total) and Fe(II).

Mössbauer spectroscopy. For Mössbauer analysis, samples of four GR materials and final microbial oxidation products after 19 days cultivation were filtered on 0.45 µm filter papers, embedded in Kapton tape in an anoxic glovebox (100 % N_2) and stored in anoxic glass bottles at -20 °C until analysis. The samples were measured at 140 K using a ^{57}Fe Mössbauer spectrometer (WissEL) with a ^{57}Co/Rh source. Spectra were fitted using the Voigt based fitting (VBF) routine in the Recoil software (University of Ottawa) (Rancourt and Ping, 1991).

Scanning electron microscopy (SEM). For SEM, culture slurry was collected and washed with ultra-pure H_2O. Washed samples were dropped on a 0.45 µm filter paper (Fig. S-2) to dry samples quickly in the glovebox and avoid chemical oxidation

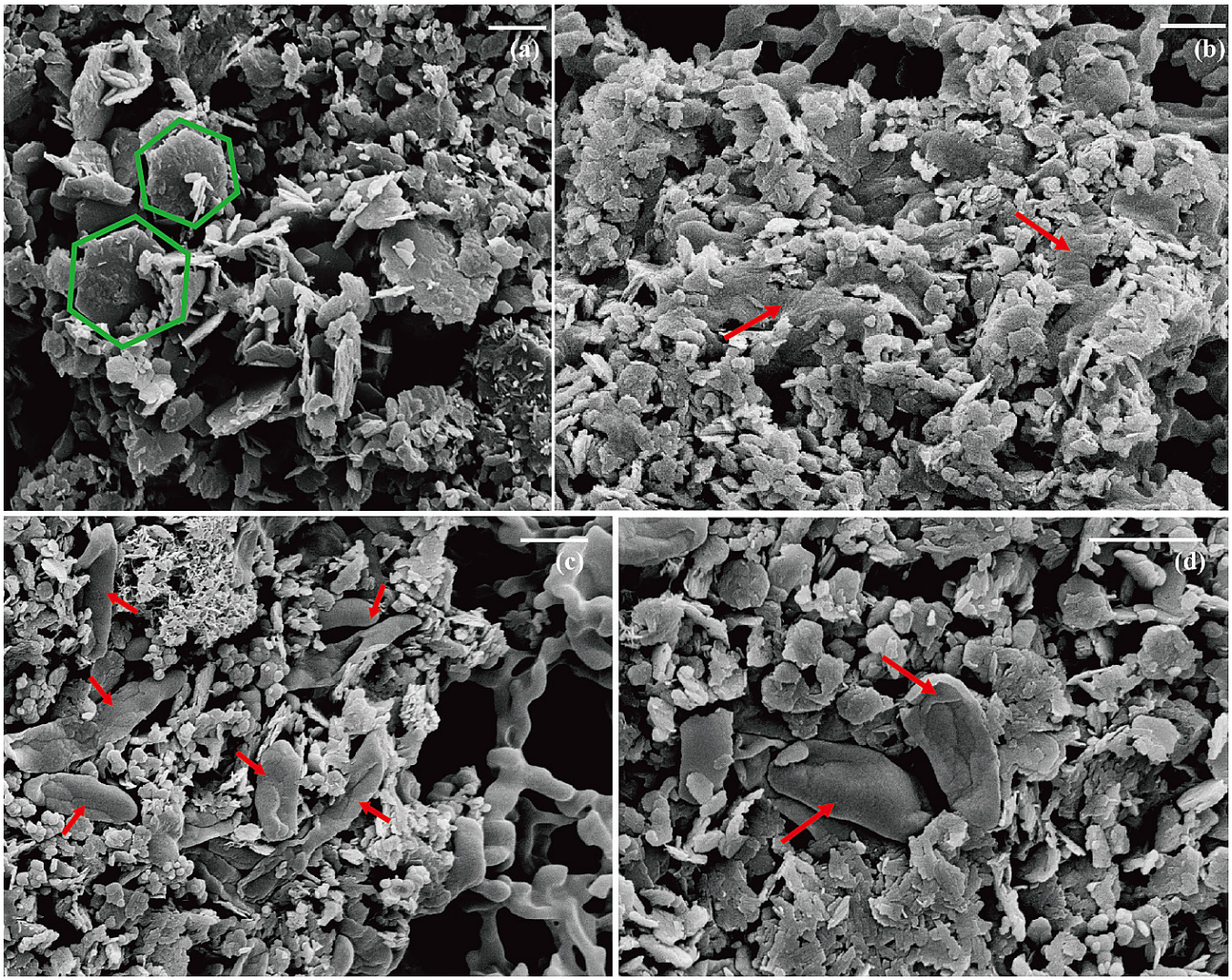

Figure 1 Scanning electron microscopy (SEM) images of **(a)** GR_SW2 starting material, **(b)** SW2 culture suspension with GR, and **(c,d)** TIE-1 culture suspension with GR after 13 days cultivation. All scale bars in figures are 1 µm. The green hexagons are GR. The red arrows point to the cells.

of samples. Dried samples were mounted onto aluminum stubs using double sided carbon tape, and coated with a 12 nm platinum (Baltec SCD005). Micrographs were collected using a JEOL JSM-6500F field emission SEM with a Schottky field emitter, acceleration voltage 5 kV, working distance 10 mm.

Results and Discussion

GR properties. Chemical dissolution followed by a spectrophotometric ferrozine assay (Stookey, 1970) showed that there was almost no Fe(II) (<0.16 mM) in the aqueous phase for the four GR materials after washing (Table 1). It should be noted, however, that more Fe was removed from initial GR by washing with SW2 and TIE-1 medium than by water, and that the pH of GR_SW2 and GR_TIE-1 were lower than initial GR and GR_water. Nevertheless, the Fe(III)/Fe(II) molar ratio in the solid phase of the four GR materials was the same (~0.3), which was consistent with Mössbauer spectroscopy (Fig. S-1). Mössbauer spectroscopy of the initial materials indicated the presence of a minor sextet phase for initial GR, GR_water and GR_TIE-1, likely goethite, and resulted from partial oxidation (3.3-13.1 %) of GR before inoculation of bacteria. SEM showed hexagonal crystals of GR_SW2 with diameter of ~1 µm (Fig. 1a), before and after washing, implying that washing with medium did not change the mineral morphology of GR.

Table 1 Fe concentration and pH of four GR materials: Initial GR, GR_water, GR_SW2 and GR_TIE-1.

GR materials	Aqueous phase	Solid phase			Total Fe(II) (mM)	Total Fe (mM)	pH
	Fe(II) (mM)	Fe(II) (mM)	Fe(III) (mM)	Fe(III) / Fe(II)			
Initial GR	0.08	140.72	41.71	0.30	140.80	182.51	9.72
GR_water	0.03	130.15	39.04	0.30	130.18	169.22	9.69
GR_SW2	0.11	108.31	31.88	0.29	108.42	140.30	8.69
GR_TIE-1	0.16	107.85	32.63	0.30	108.01	140.64	8.55

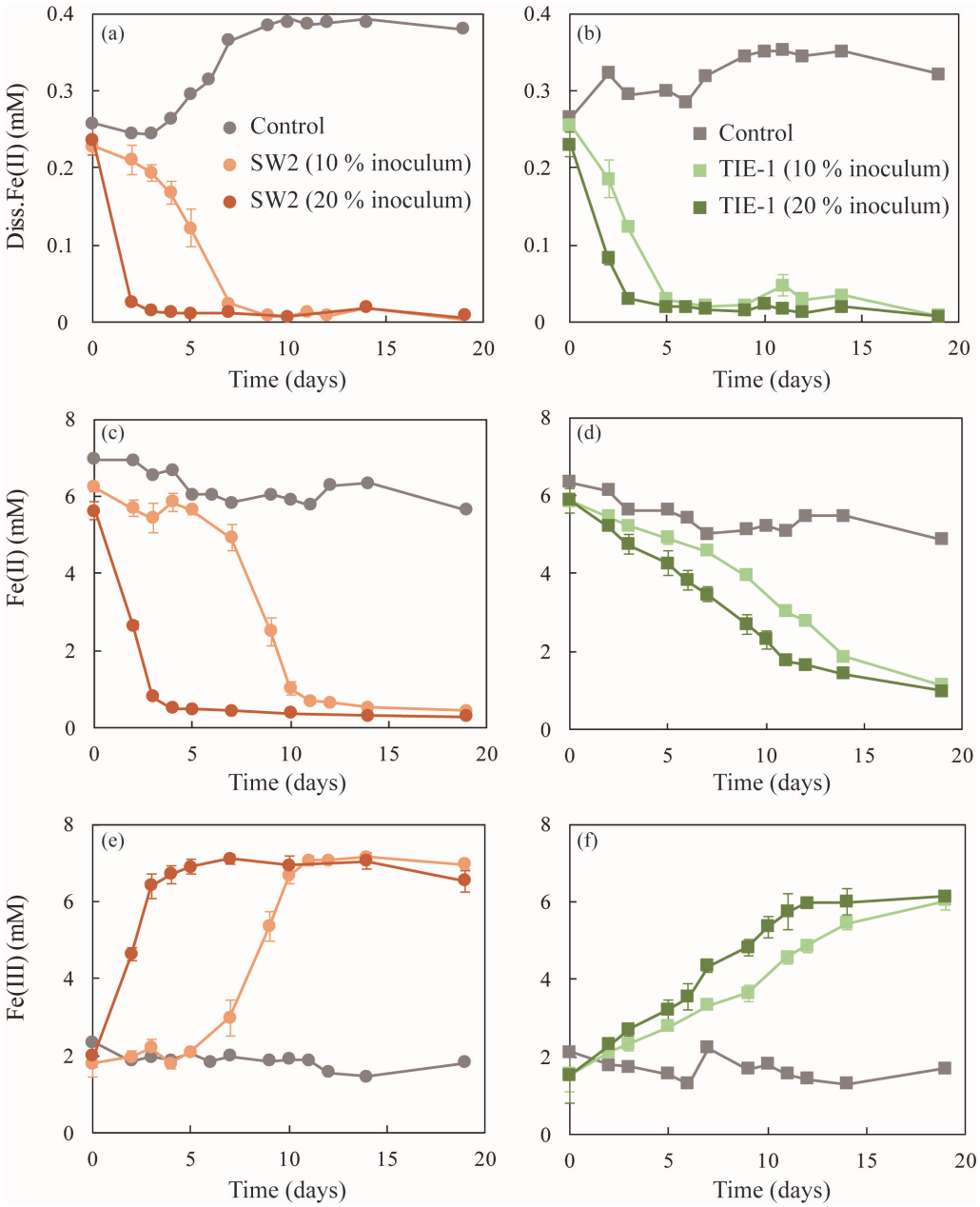

Figure 2 **(a,b)** Dissolved Fe(II), **(c,d)** Fe(II) in solid phase, **(e,f)** Fe(III) in solid phase at different time points during GR oxidation by SW2 and TIE-1. Error bars indicate standard deviation of three biological replicates.

GR oxidation rates and extent. Microcosms were set up containing GR minerals with ~6 mM Fe(II) and either strain SW2 or TIE-1. SW2 with 10 % or 20 % inoculum finished GR oxidation in 11 days or 4 days, and oxidised 89 % or 91 % solid Fe(II), respectively. The GR oxidation rate by SW2 with 20 % inoculum (1.33 mM/day) is more than twice as high as that with 10 % inoculum (0.52 mM/day). Conversely, TIE-1 with 10 % or 20 % inoculum oxidised 81 % or 83 % Fe(II) at similar rates (0.26-0.27 mM/day) during 19 days cultivation (Fig. 2). For both SW2 and TIE-1, there was still some Fe(II) left (9-19 %) in the solid phase. However, Mössbauer spectroscopy could not conclusively identify the Fe(II) phase. The Fe(II) oxidation rate determined for strain SW2 is consistent with a previous study, which hypothesised that anoxygenic phototrophs provide the most likely explanation for IF deposition in a stratified ancient ocean and the absence of Fe in Precambrian surface waters (Kappler *et al.*, 2005). Although we observed slight increases in dissolved Fe(II) (0.05-0.12 mM) and a decrease in solid phase Fe(II) (1.34-1.46 mM) in abiotic controls, this suggests only minor changes in Fe speciation including GR dissolution but not abiotic oxidation of GR.

GR oxidation products and oxidation mechanism. Mössbauer spectroscopy results showed both SW2 and TIE-1 oxidised the GR to a short range ordered Fe(III) oxyhydroxide phase. Based on hyperfine parameters, this phase is most likely to be ferrihydrite (Murad and Cashion, 2004) (Fig. 3). The minor sextet observed in the spectra of the oxidation products is likely indicative of goethite. Additionally, there was less Fe(II) remaining in the solid phase for SW2 compared to TIE-1, which is consistent with the spectrophotometric results. We observed that the rate of GR-Fe(II) oxidation was faster for SW2 than TIE-1, however, the exact reason for this is currently unknown. It has been previously shown that both strains have different mechanisms for Fe(II) oxidation *i.e.* they both use different proteins, and that affects the rate at which they are able to oxidised complexed Fe(II) (Peng *et al.*, 2019a,b). Potentially, this difference in proteins is responsible for the differences we saw here. For abiotic O_2-driven GR oxidation, where GR and dissolved oxygen are the reactants, FeOOH is the mineral end product and $[(Fe^{II})_2(Fe^{III})]$ the intermediate species. The transformation is a dissolution-oxidation-precipitation reaction (Legrand *et al.*, 2004). The dissolved

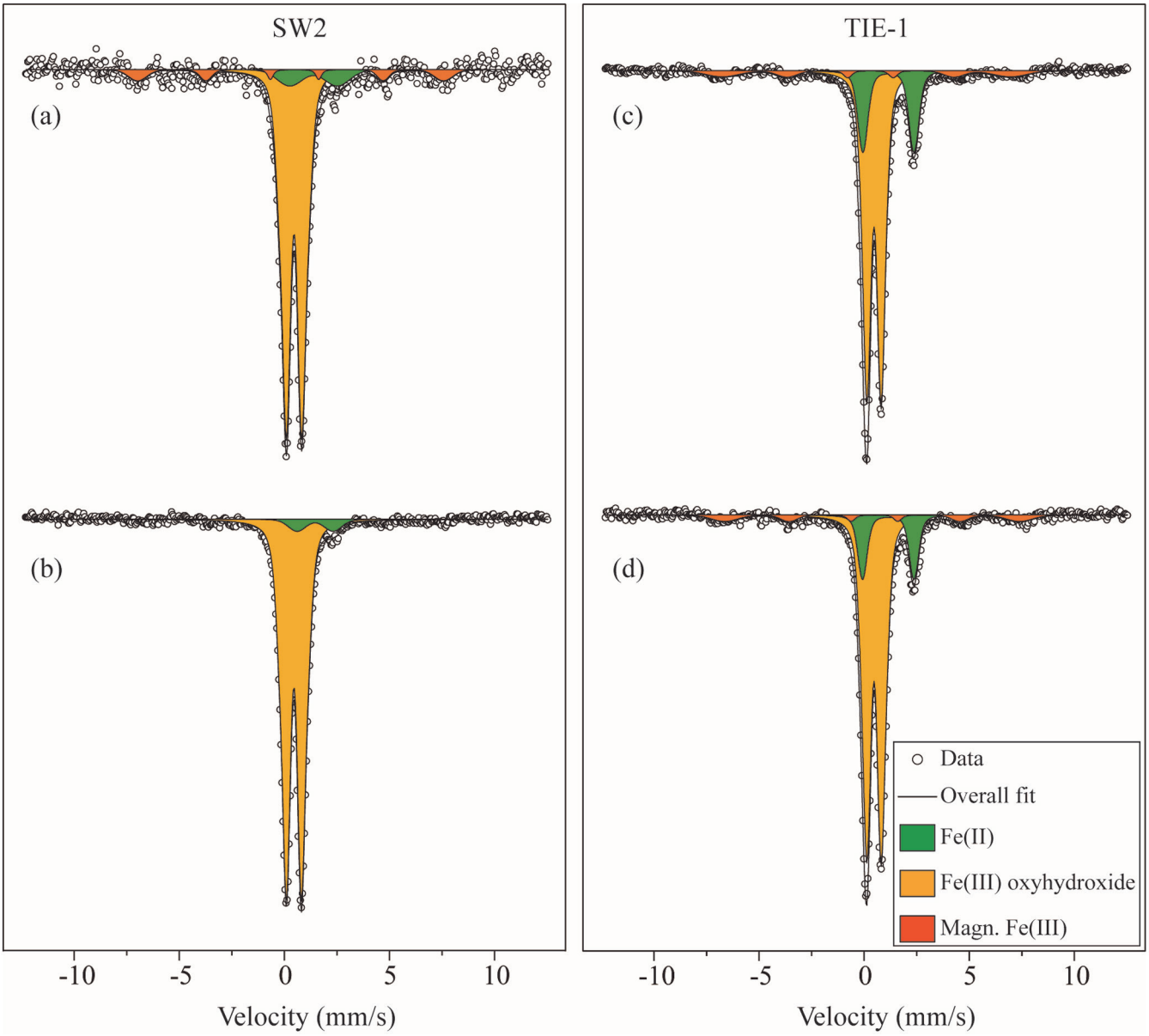

Figure 3 Mössbauer spectroscopy data of the minerals produced by oxidation of GR by the phototrophic Fe(II)-oxidising strains SW2 (10 % inoculum **(a)** and 20 % inoculum **(b)**) and TIE-1 (10 % inoculum **(c)** and 20 % inoculum **(d)**), respectively. Magn. Fe(III) corresponds to a magnetically ordered Fe mineral.

$[(Fe^{II})_2(Fe^{III})]$ species, which is in equilibrium with the GR mineral particles, is released when GR minerals dissolve as illustrated by the following schematic reaction Eq. 1 (Misawa *et al.*, 1973, 1974). In our microbial microcosm experiments with GR, the SW2 and TIE1 strains can either oxidise structural Fe(II) in GR, or these strains promote GR dissolution to Fe(II)-Fe(III) complexes or colloids, and then oxidise these more bioavailable species immediately. Obviously no complete dissolution of the GR took place since there were almost no aqueous Fe(III) and Fe(II) species (<0.03 mM) detected for SW2 and TIE-1 after 7 days and 5 days, respectively. This suggests that the reaction proceeds following Eq. 1 and Eq. 2:

$$[Fe_4^{II}Fe_2^{III}(OH)_{12}][CO_3, 2H_2O] \xleftrightarrow{\text{dissolution/precipitation}} 2[(Fe^{II})_2(Fe^{III})] + 12\ OH^- + CO_3^{2-} + 2H_2O \quad \text{Eq. 1}$$

$$2[(Fe^{II})_2(Fe^{III})]^{7+} + HCO_3^- + 10H_2O \overset{h\nu}{\Rightarrow} 6FeOOH + (CH_2O) + 13H^+ \quad \text{Eq. 2}$$

Despite reported studies on oxidation of GR by nitrate reducing Fe(II)-oxidising bacteria (Pantke *et al.*, 2012; Etique *et al.*, 2014; Miot *et al.*, 2014), the question remains whether phototrophic Fe(II)-oxidising bacteria can access lattice Fe(II) in GR. Genetic studies have shown that *pioABC* or *foxEYZ* operons are involved in electron uptake from Fe(II) by TIE-1 and SW2, respectively (Croal *et al.*, 2007; Jiao and Newman, 2007). Although SW2 could not oxidise solid phase Fe(II) mineral phases such as vivianite, magnetite or pyrite (Kappler and Newman, 2004), strain TIE-1 can access not only dissolved $[Fe^{2+}_{(aq)}]$ or complexed Fe(II) [*e.g.*, Fe(II)-nitrilotriacetic acid], but also Fe(II) in the mixed-valent Fe(II)-Fe(III) mineral magnetite (Byrne *et al.*, 2015) as well as poised electrodes (Bose *et al.*, 2014). Follow up studies have shown that for magnetite oxidation by TIE-1, a direct surface-mineral contact mechanism might be required (Byrne *et al.*, 2016). Since we did not fix cells for electron microscopy analyses, most SW2 cells appeared flattened or were difficult to distinguish from minerals (Fig. 1b), but many TIE-1 cells which have a length of ~1 µm and direct contact with the minerals could be observed (Fig 1c,d). In our study, the initial Fe(II)/Fe(III) ratio of GR was six times higher than magnetite, suggesting that if solid Fe(II) can be accessed by the bacteria, GR could potentially act as an electron donor for phototrophic Fe(II)-oxidisers. Moreover, the high solubility of GR phases could cause the Fe(II) in GR to be more bioavailable than structural Fe(II) in magnetite to phototrophic Fe(II)-oxidising bacteria through *pioABC* or *foxEYZ* operons, either when the cells are in direct contact with the minerals or when the GR is undergoing partial dissolution.

Implications for iron mineral deposition. The deposition of Precambrian rocks has mostly been interpreted as resulting from abiotic or microbial oxidation of dissolved Fe(II) (Posth *et al.*, 2013, 2014) or by oxidation of Fe(II)-containing minerals such as green rust by abiotic processes (Li *et al.*, 2017) and/or nitrate reducing iron-oxidising bacteria (Miot *et al.*, 2014). Our present study shows that anoxygenic phototrophic Fe(II)-oxidising bacteria could also play a role in oxidation of green rust and potentially the deposition of Fe(III) (oxyhydr) oxide minerals in IFs. This work supports previous claims that anoxygenic phototrophic Fe(II)-oxidising bacteria could have played a significant role in IF deposition by promoting the precipitation of Fe(III) (oxyhydr)oxides (Posth *et al.*, 2008; Czaja *et al.*, 2013). Here, we present evidence that anoxygenic phototrophic Fe(II)-oxidising bacteria can oxidise GR to a short range ordered Fe(III) oxyhydroxide in freshwater media, further highlighting the potential role of these microorganisms in the genesis of minerals in IFs in ancient environments.

Supplementary Information

The Supplementary Information contains additional Materials and Methods, Tables with Fe(II), Fe(III), Fe(tot) concentrations over time in microbial cultures and Mössbauer spectroscopy hyperfine parameters, as well as figures for Mössbauer spectrum of four GR materials and SEM image of 0.45 µm filter paper.

Acknowledgements

This research was funded by the German Research Foundation (DFG) under grant no. KA 1736/39-1. Yongxin Pan was supported by grant of the National Natural Science Foundation of China (41621004). We also thank China Scholarship Council (CSC) for the financial support to X.H.

Editor: Liane G. Benning

Additional Information

Supplementary Information accompanies this letter at http://www.geochemicalperspectivesletters.org/article2004.

Cite this letter as: Han, X., Tomaszewski, E.J., Sorwat, J., Pan, Y., Kappler, A., Byrne, J.M. (2020) Oxidation of green rust by anoxygenic phototrophic Fe(II)-oxidising bacteria. *Geochem. Persp. Let.* 12, 52–57.

References

Bocher, F., Géhin, A., Ruby, C., Ghanbaja, J., Abdelmoula, M., Génin, J.-M.R. (2004) Coprecipitation of Fe(II–III) hydroxycarbonate green rust stabilised by phosphate adsorption. *Solid State Sciences* 6, 117-124.

Bose, A., Gardel, E.J., Vidoudez, C., Parra, E.A., Girguis, P.R. (2014) Electron uptake by iron-oxidizing phototrophic bacteria. *Nature Communications* 5, 3391.

Byrne, J.M., Klueglein, N., Pearce, C., Rosso, K.M., Appel, E., Kappler, A. (2015) Redox cycling of Fe(II) and Fe(III) in magnetite by Fe-metabolizing bacteria. *Science* 347, 1473.

Byrne, J.M., Van Der Laan, G., Figueroa, A.I., Qafoku, O., Wang, C., Pearce, C.I., Jackson, M., Feinberg, J., Rosso, K.M., Kappler, A. (2016) Size dependent microbial oxidation and reduction of magnetite nano-and micro-particles. *Scientific Reports* 6, 30969.

Croal, L.R., Jiao, Y., Newman, D.K. (2007) The fox operon from Rhodobacter strain SW2 promotes phototrophic Fe (II) oxidation in Rhodobacter capsulatus SB1003. *Journal of Bacteriology* 189, 1774-1782.

Czaja, A.D., Johnson, C.M., Beard, B.L., Roden, E.E., Li, W., Moorbath, S. (2013) Biological Fe oxidation controlled deposition of banded iron formation in the ca. 3770Ma Isua Supracrustal Belt (West Greenland). *Earth and Planetary Science Letters* 363, 192-203.

Etique, M., Jorand, F.P.A., Zegeye, A., Grégoire, B., Despas, C., Ruby, C. (2014) Abiotic Process for Fe(II) Oxidation and Green Rust Mineralization Driven by a Heterotrophic Nitrate Reducing Bacteria (Klebsiella mobilis). *Environmental Science & Technology* 48, 3742-3751.

Field, E.K., Kato, S., Findlay, A.J., MacDonald, D.J., Chiu, B.K., Luther, G.W., Chan, C.S. (2016) Planktonic marine iron oxidizers drive iron mineralization under low-oxygen conditions. *Geobiology* 14, 499-508.

Halevy, I., Alesker, M., Schuster, E.M., Popovitzbiro, R., Feldman, Y. (2017) A key role for green rust in the Precambrian oceans and the genesis of iron formations. *Nature Geoscience* 10.

Jiao, Y., Newman, D.K. (2007) The pio operon is essential for phototrophic Fe (II) oxidation in Rhodopseudomonas palustris TIE-1. *Journal of Bacteriology* 189, 1765-1773.

Kappler, A., Newman, D.K. (2004) Formation of Fe(III)-minerals by Fe(II)-oxidizing photoautotrophic bacteria 1. *Geochimica et Cosmochimica Acta* 68, 1217-1226.

Kappler, A., Newman, D.K., Konhauser, K.O., Pasquero, C. (2005) Deposition of banded iron formations by anoxygenic phototrophic Fe(II)-oxidizing bacteria. *Geology* 33, 865.

Klein, C. (2005) Some Precambrian banded iron-formations (BIFs) from around the world: Their age, geologic setting, mineralogy, metamorphism, geochemistry, and origins. *American Mineralogist* 90, 1473.

Koeksoy, E., Sundman, A., Byrne, J.M., Lohmayer, R., Planer-Friedrich, B., Halevy, I., Konhauser, K.O., Kappler, A. (2019) Formation of green rust and elemental sulfur in an analogue for oxygenated ferro-euxinic transition zones of Precambrian oceans. *Geology* 47, 211-214.

Konhauser, K.O., Hamade, T., Raiswell, R., Morris, R.C., Ferris, F.G., Southam, G., Canfield, D.E. (2002) Could bacteria have formed the Precambrian banded iron formations? *Geology* 30, 1079.

Konhauser, K.O., Planavsky, N.J., Hardisty, D.S., Robbins, L.J., Warchola, T.J., Haugaard, R., Lalonde, S.V., Partin, C.A., Oonk, P.B.H., Tsikos, H., Lyons, T.W., Bekker, A., Johnson, C.M. (2017) Iron formations: A global record of Neoarchaean to Palaeoproterozoic environmental history. *Earth-Science Reviews* 172, 140-177.

Legrand, L., Mazerolles, L., Chaussé, A. (2004) The oxidation of carbonate green rust into ferric phases:solid-state reaction or transformation via solution11Associate editor: G. Sposito. *Geochimica et Cosmochimica Acta* 68, 3497-3507.

Li, Y.L., Konhauser, K.O., Zhai, M. (2017) The formation of magnetite in the early Archean oceans. *Earth and Planetary Science Letters* 466, 103-114.

Miot, J., Li, J., Benzerara, K., Sougrati, M.T., Ona-Nguema, G., Bernard, S., Jumas, J.C., Guyot, F. (2014) Formation of single domain magnetite by green rust oxidation promoted by microbial anaerobic nitrate-dependent iron oxidation. *Geochimica et Cosmochimica Acta* 139, 327-343.

Misawa, T., Hashimoto, K., Shimodaira, S. (1973) Formation of Fe(II)1 Fe(III)1 intermediate green complex on oxidation of ferrous ion in neutral and slightly alkaline sulphate solutions. *Journal of Inorganic and Nuclear Chemistry* 35, 4167-4174.

Misawa, T., Hashimoto, K., Shimodaira, S. (1974) The mechanism of formation of iron oxide and oxyhydroxides in aqueous solutions at room temperature. *Corrosion Science* 14, 131-149.

Murad, E., Cashion, J. (2004) Iron oxides. In: Murad, E., Cashion, J. (Eds.) *Mössbauer spectroscopy of environmental materials and their industrial utilization*. Springer, Boston, MA, 159-188.

Pantke, C., Obst, M., Benzerara, K., Morin, G., Ona-Nguema, G., Dippon, U., Kappler, A. (2012) Green Rust Formation during Fe(II) Oxidation by the Nitrate-Reducing Acidovorax sp. Strain BoFeN1. *Environmental Science & Technology* 46, 1439-1446.

Peng, C., Bryce, C., Sundman, A., Borch, T., Kappler, A. (2019a) Organic Matter Complexation Promotes Fe(II) Oxidation by the Photoautotrophic Fe(II)-Oxidizer Rhodopseudomonas palustris TIE-1. *ACS Earth and Space Chemistry* 3, 531-536.

Peng, C., Bryce, C., Sundman, A., Kappler, A. (2019b) Cryptic Cycling of Complexes Containing Fe(III) and Organic Matter by Phototrophic Fe(II)-Oxidizing Bacteria. *Applied and Environmental Microbiology* 85, e02826-18.

Porsch, K., Kappler, A. (2011) FeII oxidation by molecular O2 during HCl extraction. *Environmental Chemistry* 8, 190-197.

Posth, N.R., Hegler, F., Konhauser, K.O., Kappler, A. (2008) Alternating Si and Fe deposition caused by temperature fluctuations in Precambrian oceans. *Nature Geoscience* 1, 703-708.

Posth, N.R., Konhauser, K.O., Kappler, A. (2013) Microbiological processes in banded iron formation deposition. *Sedimentology* 60, 1733-1754.

Posth, N.R., Canfield, D.E., Kappler, A. (2014) Biogenic Fe(III) minerals: From formation to diagenesis and preservation in the rock record. *Earth-Science Reviews* 135, 103-121.

Rancourt, D.G., Ping, J.Y. (1991) Voigt-based methods for arbitrary-shape static hyperfine parameter distributions in Mössbauer spectroscopy. *Nuclear Instruments and Methods in Physics Research Section B: Beam Interactions with Materials and Atoms* 58, 85-97.

Refait, P., Memet, J.B., Bon, C., Sabot, R., Génin, J.M.R. (2003) Formation of the Fe(II)–Fe(III) hydroxysulphate green rust during marine corrosion of steel. *Corrosion Science* 45, 833-845.

Stookey, L.L. (1970) Ferrozine---a new spectrophotometric reagent for iron. *Analytical Chemistry* 42, 779-781.

Trolard, F., Génin, J.M.R., Abdelmoula, M., Bourrié, G., Humbert, B., Herbillon, A. (1997) Identification of a green rust mineral in a reductomorphic soil by Mossbauer and Raman spectroscopies. *Geochimica et Cosmochimica Acta* 61, 1107-1111.

Wu, W., Swanner, E.D., Hao, L., Zeitvogel, F., Obst, M., Pan, Y., Kappler, A. (2014) Characterization of the physiology and cell–mineral interactions of the marine anoxygenic phototrophic Fe(II) oxidizer Rhodovulum iodosum – implications for Precambrian Fe(II) oxidation. *FEMS Microbiology Ecology* 88, 503-515.

Xiong, J. (2007) Photosynthesis: what color was its origin? *Genome Biology* 7, 245.

Zegeye, A., Bonneville, S., Benning, L.G., Sturm, A., Fowle, D.A., Jones, C., Canfield, D.E., Ruby, C., MacLean, L.C., Nomosatryo, S., Poulton, S.W., Crowe, S.A. (2012) Green rust formation controls nutrient availability in a ferruginous water column. *Geology* 40, 599-602.